Heritability of the effective connectivity in the resting-state default mode network

Junhai Xu[1,2,3], Xuntao Yin[2], Haitao Ge[2], Yan Han[4] , Zengchang Pang[5], Yuchun Tang[2], Baolin Liu[1*], Shuwei Liu[2*], Karl Friston[3]

[1]School of Computer Science and Technology, Tianjin University, Tianjin 300072, P.R.China

[2]Research Center for Sectional and Imaging Anatomy, Shandong University School of Medicine, Jinan, Shandong, China

3Wellcome Trust Centre for Neuroimaging, University College London (UCL) Institute of Neurology, London, United Kingdom

[4]Department of Radiology, Affiliated Hospital of Medical College, Qingdao University, Qingdao, Shandong, China

[5]Department of Epidemiology, Qingdao Municipal Central for Disease Control and Prevention, Qingdao, Shandong, China

* Correspondence: Prof. Shuwei Liu, Research Center for Sectional and Imaging Anatomy, Shandong University School of Medicine, Jinan, Shandong, 250012, China. Telephone: +86-531-88382093. Fax: +86-531-88563495.

E-mail address: liusw@sdu.edu.cn

ABSTRACT

The default mode network (DMN) is thought to reflect endogenous neural activity, which is considered as one of the most intriguing phenomena in cognitive neuroscience. Previous studies have found that key regions within the DMN are highly interconnected. Here, we characterized genetic influences on causal or directed information flow within the DMN during the resting state. In this study, we recruited forty-six pairs of twins and collected fMRI imaging data using a 3.0T scanner. Dynamic causal modelling was conducted for each participant, and a structural equation model was used to calculate the heritability of default mode network in terms of its effective connectivity. Model comparison favored a full-connected model. The ACE model was preferred in the comparison of structural equation models. Heritability of DMN effective connectivity was 0.54. Establishing the heritability of default-mode effective connectivity endorses the use of resting-state networks as endophenotypes or intermediate phenotypes in the search for the genetic basis of psychiatric or neurological illnesses.

Keywords: resting state fMRI; default mode network; DCM; effective connectivity; heritability

INTRODUCTION

Spontaneous low frequency fluctuations in resting-state blood oxygenation level-dependent (BOLD) signals are thought to reflect coherent neuronal activity, which can be measured by functional magnetic resonance imaging (fMRI) (Biswal et al., 1997). These fluctuations give rise to a series of structured functional networks (Greicius et al., 2003; Fox and Raichle, 2007). Using functional connectivity analysis of fMRI or positron emission tomography (PET), a set of resting state networks have been identified and associated with distributed networks engaged during cognitive behaviors (Smith et al., 2009). The default mode network (DMN), whose activity is maximum at rest and suppressed during passive tasks, has been considered and important network in the human brain. It reflects intrinsic or endogenous neural activity and may have a role in monitoring the external environment and supporting internal mentation (Gusnard et al., 2001; Gilbert et al., 2007). Cortical regions in this network include the posterior cingulate gyrus (PCC), retrosplenial cortex and precuneus, medial prefrontal cortex (mPFC), medial/inferior temporal cortex, medial/inferior parietal cortex, and cerebellar areas (Raichle et al., 2001; Damoiseaux et al., 2006). The DMN is prevalent in normal populations (Anticevic et al., 2012) and alterations within the network have been reported in normal aging (Sheline et al., 2010; Toussaint et al., 2014). Furthermore, changes in the DMN are also found in neuropsychiatric disorders, such as Alzheimer's disease (Zhong et al., 2014; Dipasquale et al., 2015), depression (Sheline et al., 2009; Liston et al., 2014), schizophrenia (Calhoun et al., 2008; Tang et al., 2013; Pankow et al., 2015), and amnestic mild cognitive disorders (Wang et al., 2013; Weiler et al., 2014).

The spatial pattern of the DMN may be inherent to the mammalian brain, because it is present in sleeping babies (Fransson et al., 2007; Schopf et al., 2012) and nonhuman primates (Vincent et al., 2007). Many studies have showed that spontaneous fluctuations in resting state are subject to significant genetic effects; suggesting that they could serve as endophenotypes or intermediate phenotypes in search for the genetic origins of brain disorders (Glahn et al., 2010; Fornito et al., 2011; Korgaonkar

et al., 2014). The genetic influence on regional coactivation and ensuing functional connectivity of DMN has been found in normal subjects (Karlsgodt et al., 2010) , and subjects with psychiatric disorders, such as Alzheimer's disease (Persson et al., 2008), schizophrenia (Whitfield-Gabrieli et al., 2009; Meda et al., 2014) and major depressive disorder (Rao et al., 2007).

Twin studies using both monozygotic (MZ) and dizygotic (DZ) twins provide a unique opportunity to explore the genetic and environmental influences, not only on the variation of individual trait but also on cross-trait correlations. Moreover, study designs involving pedigrees and twins can provide evidence for gene-environment interactions (Purcell, 2002). Such evidence may illuminate molecular, neuropsychiatric and epidemiological studies of the pathophysiology of disease processes. Previous studies have explored the genetic and environmental influences on the activity and functional connectivity of the DMN. However, it remains unclear how genetic and environment effects impact on the effective (directed) connectivity within the DMN.

Functional connectivity is defined as the statistical dependence among remote neurophysiological events. It usually rests on measures like correlations, coherence, or transfer entropy to describe these dependencies (Friston, 2011). Mechanistically, the integration of a distributed system can be better understood in terms of effective connectivity: effective connectivity quantifies the directed coupling among brain regions, while functional connectivity reflects (undirected) statistical associations. Effective connectivity refers to the influence that one neural system exerts over another. One technique, called dynamic causal modeling (DCM), has been developed to analyze effective connectivity (Friston et al., 2003), and recently stochastic DCM has been proposed to model spontaneous fluctuations in BOLD signals and estimate effective connectivity in the absence of a experimental manipulation (Li et al., 2011). In short, analyses of effective connectivity, using DCM, enable us to make inferences about the hidden information flow in a distributed network by comparing the evidence for different models (i.e. directed graphs or architectures) of coupling.

Based on previous findings of significant genetic influence on the functional

connectivity of the DMN (Glahn et al., 2010; Korgaonkar et al., 2014), we hypothesized that genetics make a significant contribution to the effective connectivity within DMN. To identify the contribution of genetic and environment effects, the current study quantified the effective connectivity within DMN at rest using fMRI. Group independent component analysis (ICA) analyses were first performed to decompose the functional data into spatially independent components. Then the default mode was identified through a canonical template, and four representative ROIs were defined for further (stochastic) DCM analysis. After estimating the effective connectivity between four ROIs using stochastic DCM, a structural equation model was used to calculate the heritability of the effective connectivity within DMN.

MATERIALS AND METHODS

Participants

24 (13 male and 11 female) monozygotic (MZ) and 22 (12 male and 10 female) dizygotic (DZ) twin pairs (mean age = 17.13, SD = 1.58; range from 15-20 years old) were recruited from the Qingdao Twin Registry, established in 1998 at the Qingdao Center for Disease Control and Prevention (Duan et al., 2013). Inclusion criteria were: (1) right-handed measured with the Edinburgh handedness inventory (Oldfield, 1971); (2) no history of any neurological or psychiatric disorders, or cognitive complaints, and no abnormal findings observed in conventional brain MRI. Venous blood was drawn for zygosity identification (for like-sex twin pairs) using 16 multiple short tandem sequence repeated DNA markers at the center laboratory of Qingdao Blood Center, with the zygosity assignment ascertained to be 99.9%.

The study was supported and approved by the Human Research Ethics Committee of Shandong University School of Medicine. Written informed consents were obtained from all participants, as well as their parents.

Data acquisition

All participants were scanned using a 3.0 Tesla GE Signa scanner (General Electric

Medical Systems, Milwaukee, WI), with a standard eight-channel head coil. To reduce head motion and scanner noise during scanning, foam pads and earplugs were used to stabilize each participants' heads. Subjects were instructed to keep their eyes closed, relax and think of nothing in particular (without falling asleep). The functional MR images were obtained using an echo-planar imaging (EPI) sequence: 35 axial slices, thickness/gap= 3.5 / 0.7 mm, matrix= 64×64, repetition time (TR) = 2000 ms, echo time (TE) = 35 ms, flip angle (FA) = 90°, field of view (FOV) = 224×224 mm^2. The scan lasted for 5 min 42 s, during which time 171 images were collected for each subject.

In addition, a three-dimensional volume spoiled gradient-echo (SPGR) pulse sequence with 174 slices (TR = 6.5 ms, TE = 2.0 ms, thickness /gap= 1.0 / 0 mm, matrix = 256×256, FOV = 256×256 mm^2, FA = 15°) was used to acquire the high-resolution T1-weighted images for anatomical reference.

Image preprocessing

Image preprocessing was conducted using SPM8 software (*http://www.fil.ion.ucl.ac.uk/spm/*). The first 10 volumes for each participant were discarded to allow for T1 equilibration effects and adaptation of participants to the scanning environment. The remaining functional images were first corrected for time delay between slices and head motion. A six-parameter rigid body transformation was used to realign the functional images to the first image. As all participants' head movements were less than 1.5 mm and 1 degree, no participant was excluded. Next, the high-resolution structural image was coregistered with the functional images and was subsequently segmented. The mapping between the anatomical image and the Montreal Neurological Institute (MNI) echo-planar imaging (EPI) template was used to spatially normalize the realigned images into a standard stereotaxic space at $3 \times 3 \times 3$ mm. Finally, the functional data were spatially smoothed by convolution with an isotropic Gaussian kernel (FWHM = 4 mm) to attenuate spatial noise

Independent component analysis

To identify regions for subsequent DCM, we first identified the DMN in each subject using ICA: after data preprocessing, GICA was conducted to decompose the resting

state data into spatial ICs using the GIFT software (http://icatb.sourceforge.net/). First, the optimal components was estimated using the minimum description length criteria (Li et al., 2007), and the number was 41 in this study. Time series from all subjects were concatenated and decomposed into ICs using the infomax algorithm, resulting in 41 independent spatial maps. The corresponding components for each subject were calculated through a back reconstruction step.

We identified the default mode component automatically using a DMN template, generated using the WFU PickAtlas Tool 3.0 (http://fmri.wfubmc.edu/software/pickatlas). In current study, we created the template with the bilateral precuneus, posterior cingulate, angular, inferior parietal cortex and superior medial frontal cortex. All the spatial components were then sorted using a multiple spatial regression of the template with the ICs. The component with the highest regression coefficient was identified as the default mode component. To locate the default mode regions that were conserved over subjects, a one sample t-test was performed to produce a group-mean DMN with subject-specific default mode components.

Region of interest definition

Based on the identification of the default mode above, we defined four ROIs: the PCC, mPFC, left lateral parietal cortex (LPC) and right lateral parietal cortex (RPC). The ROIs were centered on the local maximum of the default mode component that was nearest the maxima in the group mean map. For each subject, the time series of all four ROIs were extracted from a 6 mm sphere.

Dynamic causal modelling

Effective connectivity analysis was performed using DCM10 in SPM8. Stochastic DCM tries to explain how neuronal activity in one region is affected by neuronal activity in others based on nonlinear differential equations. Distributed neuronal activity is modeled by hidden neuronal states within each region using (neuronal) state equations. The state equations also model the conversion from hidden neuronal states to observed fMRI signals via hemodynamic states, such as blood flow and deoxyhemoglobin concentration. The ensuing stochastic differential equations contain

parameters corresponding to effective connectivity mediating influences both within and between regions. Stochastic DCM can exploit spontaneous fluctuations in activity by including random fluctuations in the state equations. Each DCM contains three kinds of unknown parameters that are estimated: the parameters of the state equations, the hidden states *per se* and precision of measurement noise. Model fitting or inversion provides estimates of these quantities using standard (variational) Bayesian techniques. In this instance, generalised Bayesian filtering (Friston et al., 2010). For details, please see (Li et al., 2011).

The stochastic DCM neuronal state equations can be summarised as follows:

$$\frac{dx}{dt} = (A + \sum_{j} u_j B^{(j)})x + Cv + \omega^{(x)}$$
$$v = u + \omega^{(v)}$$

Generalised Bayesian filtering was conducted to fit a fully connected DCM for each subject. After this, the DCM results were then optimised to identify which connections where present (i.e., not redundant). In detail, our stochstic DCMs were fully and reciprocally connected generating 16 connections within and among four nodes for each subject. The full DCM was then inverted using generalised filtering. The best model was recoverd throught a Bayesian network discovery scheme –known as *post hoc* optimiztion or Bayesian model reduction (Friston et al., 2011). This estimate the model evidence and parameters for all reduced models (from which all combinations of connections are removed) using the estimates from a full model. Bayesian model averaging then provides the effective connectivity estimates for each subject.

After model reduction, singular value decomposition (SVD) analysis was used to identify the prical component or mixture of connections that showed the greatest variation over subjects. This connectivity measure was used for further genetic analysis. The SVD analysis was performed as follows:

$$\theta = \begin{bmatrix} \theta_{11} & \cdots & \theta_{1N} \\ \vdots & \ddots & \vdots \\ \theta_{M1} & \cdots & \theta_{MN} \end{bmatrix} \quad M = 92, N = 16$$

$$[U, S, V] = SVD(\theta)$$

The first column of the matrix U corresponds to the principal component of interest.

Genetic analysis

Univariate genetic modeling was used to estimate the genetic and environmental contributions to effective connectivity in DMN. Genetic modelling was performed using OpenMx (Boker et al., 2011) with a full information maximum likelihood estimator on R version 3.1.0 (R Development Core Team, 2012). There were three sets of variance in the genetic model, which included the additive genetics (A), dominant genetics (D), common environment (C) and unique environment (E). In the twin genetic analysis, we rely on the assumption that the additive and dominant genetics are 100% shared between MZ twins and 50 or 25% shared between MZ twins. Finally, the common environment is 100% shared, while the unique environment is not shared. The significance of all the contribution parameters is estimated by removing each parameter from the genetic model and then comparing the evidences of the resulting models (c.f., Bayesian model reduction). Full ACE and ADE model comparison was performed using maximum likelihood estimation. In detail, the within-group correlation was first calculated for MZ and DZ twins (r_{MZ} and r_{DZ}). When $r_{MZ} \leqq 2\, r_{DZ}$, the ACE model was selected; when $r_{MZ} > 2\, r_{DZ}$, the ADE model was selected. Model comparisons were conducted using the Akaike's Information Criterion (and log likelihood chi-square difference test). A significant change in the AIC suggests that the missing parameter accounts for a significant contribution to phenotypic variation, and should be retained. Age and gender covariates were included in the models.

RESULTS

Demographic information

In this study, we examined neuroimaging data from forty-six pairs of twins, which included twenty-four MZ (male: 13 pairs; female: 11 pairs) and twenty-two DZ (male: 12 pairs; female: 10 pairs). The average age of the sample was 17.13 years old (SD: 1.58). Independent-sample t-tests revealed that there were no significant age differences for all pairs of twins. Table 1 summarizes the demographic information of our sample.

The DCM analysis and effective connectivity of DMN

Group ICA analysis was performed on the resting state data to decompose the time series in terms of spatial pattern. Subject-specific default modes were identified using a default mode template. Figure 2 shows the mean default mode component for all the subjects. A one sample t-test was used to identify the DMN regions that were consistent across subjects. The result of the one sample t-test is shown in Figure 3A as a statistical parametric map. Based on this ICA analysis, we defined four ROIs including the PCC, mPFC, LPC and RPC. The locations of these ROIs are shown in Figure 3B, for a typical subject.

Generalized filtering was conducted to estimate the hidden states of the ROIs and their effective connectivity. Figure 4 shows the estimated neuronal and hemodynamic state of the PCC following model inversion. Figure 4A and B show the estimated hidden states, which include the neuronal activity, vasodilatory signals, normalized flow, volume and deoxyhemoglobin (dHb) content. Figure 4C depicts the predicted response and associated prediction errors. We found that the conditional expectations in neuronal activity and hemodynamic states could account for most of the observed fluctuations in the resting-state fMRI time series. Furthermore, there were low amplitude fluctuations in the predictions that comprised an estimate of noise, although the slower and larger fluctuations were well predicted.

The best model was then recovered from the estimates of the fully-connected DCM using Bayesian model reduction for each subject. Figure 5 shows the resulting

estimates. There were 6536 reduced models, for all combinations of connections between 4 ROIs. Figure 5A shows the log evidence for over all models. We can see that with more connections, the models have greater evidence. As we expected, the full-connected model exhibited the greatest evidence and was the best explanation for our data. That is to say, the model evidence would decline if any connection was removed. The 90% Bayesian confidence intervals were shown in Figure 5B. When these intervals do not contain zero, it means that the connections contribution to the model evidence was substantial. Figure 6 shows the optimized (fully connected) DCM model for one typical subject in resting state.

Heritability of the effective connectivity in DMN

After the conditional parameter estimates were computed, SVD was used for each subject to obtain the principal component of DMN connectivity for further genetic analysis. The within-group correlation coefficients were first calculated for MZ and DZ twins. We found that the correlation of MZ (r_{MZ}) was 0.72, while the correlation of DZ (r_{DZ}) was 0.48. The ACE model was the best model of phenotypic variations in effective connectivity. The heritability was significant for the effective connectivity ($V_A = 0.54$, $P < 0.001$), Table 2 summarized the ACE estimates for connectivity measures between DMN.

DISCUSSION

In this present study, we calculated the effective connectivity within the DMN in resting state, using stochastic DCM. Four ROIs (PCC, mPFC, LPC and RPC) were identified using ICA. We found that the full-connected model was the best explanation for our functional data. Subsequent genetic analysis demonstrated that genetics made a significant contribution to intersubject variations in effective connectivity of the DMN network, with a heritability of 0.54. Establishing the heritability of default-mode effective connectivity further endorses the use of resting-state effective connectivity as a potential endophenotype or intermediate endophenotype to guide the treatment and prognostication in brain diseases, and in the search for the genetic roots of brain disorders.

Resting-state effective connectivity of the DMN

The functional connectivity within DMN has received much attention; both in normal populations and subject with disorders (Rosazza and Minati, 2011). Some researchers have explored the directed functional connectivity among the DMN regions using a variety of approaches, such as Bayesian networks (Wu et al., 2011), Granger causality (Zhou et al., 2011) and partial directed coherence (Silfverhuth et al., 2011). Compared to other schemes, the advantage of DCM is that a hemodynamic model is used to estimate hidden neuronal states from observed fMRI signals. This is crucial for fMRI data, where observed BOLD signals are hemodynamic convolutions of underlying neuronal fluctuations (Li et al., 2012). In the current study, the full-connected mode was found to be the best model, in terms of model evidence. Bidirectional connections were observed between the PCC and LPC, PCC and RPC, mPFC and LPC, as well as mPFC and RPC in resting state, which is consistent with previous research on the DMN (Wu et al., 2011; Zhou et al., 2011). Directed connections between PCC and mPFC were also disclosed by our study, These two nodes play a key role in the DMN – and are both functionally and anatomically connected (Price, 2007). Finally, functional connectivity has been demonstrated between the PCC and bilateral parietal cortex in human brain, and prominent anatomical connections were also found in macaque monkey (Kobayashi and Amaral, 2007).

Heritability of the effective connectivity within DMN

The main purpose of this study was to identify the genetic and environmental contribution to resting-state effective connectivity in DMN. The heritability of the effective connectivity within DMN was 0.54, which suggested that the genes had a significant influence on the connectivity mediating spontaneous fluctuations in the resting state. Genetic effects have been shown to have a great genetic influence on resting-state functional connections in the human brain, ranging from 60% in adults (Fornito et al., 2011) to 42% in children (van den Heuvel et al., 2013). One previous pedigree study has found that 40% of the functional-connectivity variance is genetically controlled (Glahn et al., 2010). Another twin study has demonstrated that not all functional connections within DMN were significantly heritable, with the

strongest heritable influence in the functional connections between PCC and inferior parietal cortex (41% for right and 24% for left) (Korgaonkar et al., 2014). Moreover, one study on the first-degree relatives of subjects with schizophrenia provided further support for a genetic role in resting state brain activity (Whitfield-Gabrieli et al., 2009). Altered resting-state connectivity is also observed in the genetic disorders such as patients with 22q11.2 deletion syndrome (Schreiner et al., 2014). The heritability of effective connectivity in DMN was lower than that in adults, but higher than that in children, which is reasonable as the subjects in this study were adolescence.

Moreover, recent studies have investigated the role of specific genes in the regulation of DMN connectivity. Catechol-O-methyl transferase (COMT) and brain-derived neurotrophic factor (BDNF) single nucleotide polymorphisms have been demonstrated to be associated with altered functional connectivity within the DMN, and there are links between COMT and BDNF to psychiatric disorders like depression (Arlt et al., 2013). Given the discovery of altered DMN in both mild cognitive impairment and Alzheimer's disease, these findings provide evidence that resting state connections may be an early biomarker of genetic risk (Filippini et al., 2009). The genetic contribution to effective connectivity in our study suggests that this measure may serve as a potential endophenotype for exploring the genetic origins of brain disorders.

LIMITATIONS

There are some limitations to be acknowledged in this study. First, the sample in our study is in adolescents: with increasing age, there may be some changes in their default mode network. We also included age as a covariate in the genetic analysis, which could ensure the robustness of our result to some extent. Second, the sample was relatively small, which could reduce statistical efficiency. Future studies should increase sample size to ensure more efficient results.

CONCLUSIONS

In this study, we quantified the effective connectivity within the DMN in resting state fMRI data using stochastic DCM – and investigated the genetic and environmental

contributions to resting-state effective connectivity. We demonstrated that the effective connectivity of the DMN is under genetic control using twin genetic analysis. Establishing the heritability of default mode effective connectivity provides further support for this measure as a potential endophenotype or intermediate phenotype in the search of the genetic origins of neurological and psychiatric disorders.

ACKNOWLEDGEMENTS

REFERENCES

Anticevic A, Cole MW, Murray JD, Corlett PR, Wang XJ, Krystal JH (2012) The role of default network deactivation in cognition and disease. Trends in cognitive sciences 16:584-592.

Arlt S, Demiralay C, Tharun B, Geisel O, Storm N, Eichenlaub M, Lehmbeck JT, Wiedemann K, Leuenberger B, Jahn H (2013) Genetic risk factors for depression in Alzheimer`s disease patients. Current Alzheimer research 10:72-81.

Biswal BB, Van Kylen J, Hyde JS (1997) Simultaneous assessment of flow and BOLD signals in resting-state functional connectivity maps. NMR in biomedicine 10:165-170.

Boker S, Neale M, Maes H, Wilde M, Spiegel M, Brick T, Spies J, Estabrook R, Kenny S, Bates T, Mehta P, Fox J (2011) OpenMx: An Open Source Extended Structural Equation Modeling Framework. Psychometrika 76:306-317.

Calhoun VD, Maciejewski PK, Pearlson GD, Kiehl KA (2008) Temporal lobe and "default" hemodynamic brain modes discriminate between schizophrenia and bipolar disorder. Human brain mapping 29:1265-1275.

Damoiseaux JS, Rombouts SA, Barkhof F, Scheltens P, Stam CJ, Smith SM, Beckmann CF (2006) Consistent resting-state networks across healthy subjects. Proceedings of the National Academy of Sciences of the United States of America 103:13848-13853.

Dipasquale O, Griffanti L, Clerici M, Nemni R, Baselli G, Baglio F (2015) High-Dimensional ICA Analysis Detects Within-Network Functional Connectivity Damage of Default-Mode and Sensory-Motor Networks in Alzheimer's Disease. Frontiers in human neuroscience 9:43.

Duan H, Ning F, Zhang D, Wang S, Tan Q, Tian X, Pang Z (2013) The Qingdao Twin Registry: a status update. Twin research and human genetics : the official journal of the International Society for Twin Studies 16:79-85.

Filippini N, MacIntosh BJ, Hough MG, Goodwin GM, Frisoni GB, Smith SM, Matthews PM, Beckmann CF, Mackay CE (2009) Distinct patterns of brain activity in young carriers of the APOE-epsilon4 allele. Proceedings of the National Academy of Sciences of the United States of America 106:7209-7214.

Fornito A, Zalesky A, Bassett DS, Meunier D, Ellison-Wright I, Yucel M, Wood SJ, Shaw K, O'Connor J, Nertney D, Mowry BJ, Pantelis C, Bullmore ET (2011) Genetic influences on cost-efficient organization of human cortical functional networks. The Journal of neuroscience : the official journal of the Society for Neuroscience 31:3261-3270.

Fox MD, Raichle ME (2007) Spontaneous fluctuations in brain activity observed with functional magnetic resonance imaging. Nature reviews Neuroscience 8:700-711.

Fransson P, Skiold B, Horsch S, Nordell A, Blennow M, Lagercrantz H, Aden U (2007) Resting-state networks in the infant brain. Proceedings of the National Academy of Sciences of the United States of America 104:15531-15536.

Friston K, Stephan K, Li B, Daunizeau J (2010) Generalised filtering. Math Probl Eng 2010:1-35.

Friston KJ (2011) Functional and effective connectivity: a review. Brain connectivity 1:13-36.

Friston KJ, Harrison L, Penny W (2003) Dynamic causal modelling. NeuroImage 19:1273-1302.

Friston KJ, Li B, Daunizeau J, Stephan KE (2011) Network discovery with DCM. NeuroImage 56:1202-1221.

Gilbert SJ, Dumontheil I, Simons JS, Frith CD, Burgess PW (2007) Comment on "Wandering minds: the default network and stimulus-independent thought". Science 317:43; author reply 43.

Glahn DC, Winkler AM, Kochunov P, Almasy L, Duggirala R, Carless MA, Curran JC, Olvera RL, Laird AR, Smith SM, Beckmann CF, Fox PT, Blangero J (2010) Genetic control over the resting brain. Proceedings of the National Academy of Sciences of the United States of America 107:1223-1228.

Greicius MD, Krasnow B, Reiss AL, Menon V (2003) Functional connectivity in the resting brain: a network analysis of the default mode hypothesis. Proceedings of the National Academy of Sciences of the United States of America 100:253-258.

Gusnard DA, Akbudak E, Shulman GL, Raichle ME (2001) Medial prefrontal cortex and self-referential mental activity: relation to a default mode of brain function. Proceedings of the National Academy of Sciences of the United States of America 98:4259-4264.

Karlsgodt KH, Kochunov P, Winkler AM, Laird AR, Almasy L, Duggirala R, Olvera RL, Fox PT, Blangero J, Glahn DC (2010) A multimodal assessment of the genetic control over working memory. The Journal of neuroscience : the official journal of the Society for Neuroscience 30:8197-8202.

Kobayashi Y, Amaral DG (2007) Macaque monkey retrosplenial cortex: III. Cortical efferents. The Journal of comparative neurology 502:810-833.

Korgaonkar MS, Ram K, Williams LM, Gatt JM, Grieve SM (2014) Establishing the resting state default mode network derived from functional magnetic resonance imaging tasks as an endophenotype: A twins study. Human brain mapping 35:3893-3902.

Li B, Wang X, Yao S, Hu D, Friston K (2012) Task-Dependent Modulation of Effective Connectivity within the Default Mode Network. Frontiers in psychology 3:206.

Li B, Daunizeau J, Stephan KE, Penny W, Hu D, Friston K (2011) Generalised filtering and stochastic DCM for fMRI. NeuroImage 58:442-457.

Li YO, Adali T, Calhoun VD (2007) Estimating the number of independent components for functional magnetic resonance imaging data. Human brain mapping 28:1251-1266.

Liston C, Chen AC, Zebley BD, Drysdale AT, Gordon R, Leuchter B, Voss HU, Casey BJ, Etkin A, Dubin MJ (2014) Default mode network mechanisms of transcranial magnetic stimulation in depression. Biological psychiatry 76:517-526.

Meda SA, Ruano G, Windemuth A, O'Neil K, Berwise C, Dunn SM, Boccaccio LE, Narayanan B, Kocherla M, Sprooten E, Keshavan MS, Tamminga CA, Sweeney JA, Clementz BA, Calhoun VD, Pearlson GD (2014) Multivariate analysis reveals genetic associations of the resting default mode network in psychotic bipolar disorder and schizophrenia. Proceedings of the National Academy of Sciences of the United States of America 111:E2066-2075.

Oldfield RC (1971) The assessment and analysis of handedness: the Edinburgh inventory. Neuropsychologia 9:97-113.

Pankow A, Deserno L, Walter M, Fydrich T, Bermpohl F, Schlagenhauf F, Heinz A (2015) Reduced default mode network connectivity in schizophrenia patients. Schizophrenia research.

Persson J, Lind J, Larsson A, Ingvar M, Sleegers K, Van Broeckhoven C, Adolfsson R, Nilsson LG, Nyberg L (2008) Altered deactivation in individuals with genetic risk for Alzheimer's disease. Neuropsychologia 46:1679-1687.

Price JL (2007) Definition of the orbital cortex in relation to specific connections with limbic and visceral structures and other cortical regions. Annals of the New York Academy of Sciences 1121:54-71.

Purcell S (2002) Variance components models for gene-environment interaction in twin analysis. Twin research : the official journal of the International Society for Twin Studies 5:554-571.

Raichle ME, MacLeod AM, Snyder AZ, Powers WJ, Gusnard DA, Shulman GL (2001) A default mode of brain function. Proceedings of the National Academy of Sciences of the United States of America 98:676-682.

Rao H, Gillihan SJ, Wang J, Korczykowski M, Sankoorikal GM, Kaercher KA, Brodkin ES, Detre JA, Farah MJ (2007) Genetic variation in serotonin transporter alters resting brain function in healthy individuals. Biological psychiatry 62:600-606.

Rosazza C, Minati L (2011) Resting-state brain networks: literature review and clinical applications. Neurological sciences : official journal of the Italian Neurological Society and of the Italian Society of Clinical Neurophysiology 32:773-785.

Schopf V, Kasprian G, Brugger PC, Prayer D (2012) Watching the fetal brain at 'rest'. International journal of developmental neuroscience : the official journal of the International Society for Developmental Neuroscience 30:11-17.

Schreiner MJ, Karlsgodt KH, Uddin LQ, Chow C, Congdon E, Jalbrzikowski M, Bearden CE (2014) Default mode network connectivity and reciprocal social behavior in 22q11.2 deletion syndrome. Social cognitive and affective neuroscience 9:1261-1267.

Sheline YI, Raichle ME, Snyder AZ, Morris JC, Head D, Wang S, Mintun MA (2010) Amyloid plaques disrupt resting state default mode network connectivity in cognitively normal elderly. Biological psychiatry 67:584-587.

Sheline YI, Barch DM, Price JL, Rundle MM, Vaishnavi SN, Snyder AZ, Mintun MA, Wang S, Coalson RS, Raichle ME (2009) The default mode network and self-referential processes in depression. Proceedings of the National Academy of Sciences of the United States of America 106:1942-1947.

Silfverhuth MJ, Remes J, Starck T, Nikkinen J, Veijola J, Tervonen O, Kiviniemi V (2011) Directional connectivity of resting state human fMRI data using cascaded ICA-PDC analysis. Acta Radiol 52:1037-1042.

Smith SM, Fox PT, Miller KL, Glahn DC, Fox PM, Mackay CE, Filippini N, Watkins KE, Toro R, Laird AR, Beckmann CF (2009) Correspondence of the brain's functional architecture during activation and rest. Proceedings of the National Academy of Sciences of the United States of America 106:13040-13045.

Tang J, Liao Y, Song M, Gao JH, Zhou B, Tan C, Liu T, Tang Y, Chen J, Chen X (2013) Aberrant default mode functional connectivity in early onset schizophrenia. PloS one 8:e71061.

Toussaint PJ, Maiz S, Coynel D, Doyon J, Messe A, de Souza LC, Sarazin M, Perlbarg V, Habert MO, Benali H (2014) Characteristics of the default mode functional connectivity in normal ageing and Alzheimer's disease using resting state fMRI with a combined approach of entropy-based and graph theoretical measurements. NeuroImage 101:778-786.

van den Heuvel MP, van Soelen IL, Stam CJ, Kahn RS, Boomsma DI, Hulshoff Pol HE (2013) Genetic control of functional brain network efficiency in children. European neuropsychopharmacology : the journal of the European College of Neuropsychopharmacology 23:19-23.

Vincent JL, Patel GH, Fox MD, Snyder AZ, Baker JT, Van Essen DC, Zempel JM, Snyder LH, Corbetta M, Raichle ME (2007) Intrinsic functional architecture in the anaesthetized monkey brain. Nature 447:83-86.

Wang L, Li H, Liang Y, Zhang J, Li X, Shu N, Wang YY, Zhang Z (2013) Amnestic mild cognitive impairment: topological reorganization of the default-mode network. Radiology 268:501-514.

Weiler M, Teixeira CV, Nogueira MH, de Campos BM, Damasceno BP, Cendes F, Balthazar ML (2014) Differences and the relationship in default mode network intrinsic activity and functional connectivity in mild Alzheimer's disease and amnestic mild cognitive impairment. Brain connectivity 4:567-574.

Whitfield-Gabrieli S, Thermenos HW, Milanovic S, Tsuang MT, Faraone SV, McCarley RW, Shenton ME, Green AI, Nieto-Castanon A, LaViolette P, Wojcik J, Gabrieli JD, Seidman LJ (2009) Hyperactivity and hyperconnectivity of the default network in schizophrenia and in first-degree relatives of persons with schizophrenia. Proceedings of the National Academy of Sciences of the United States of America 106:1279-1284.

Wu X, Li R, Fleisher AS, Reiman EM, Guan X, Zhang Y, Chen K, Yao L (2011) Altered default mode network connectivity in Alzheimer's disease--a resting functional MRI and Bayesian network study. Human brain mapping 32:1868-1881.

Zhong Y, Huang L, Cai S, Zhang Y, von Deneen KM, Ren A, Ren J (2014) Altered effective connectivity patterns of the default mode network in Alzheimer's disease: an fMRI study. Neuroscience letters 578:171-175.

Zhou Z, Wang X, Klahr NJ, Liu W, Arias D, Liu H, von Deneen KM, Wen Y, Lu Z, Xu D, Liu Y (2011) A conditional Granger causality model approach for group analysis in functional magnetic resonance imaging. Magnetic resonance imaging 29:418-433.

Figure legend

Figure 1. ACE genetic modeling using a twin design. Additive genetics (A), common environment (C), and unique environment (E) variables are modeled and their contributions to the variance (a, d, c, and e, respectively) of the functional connectivity measures estimated using data from each twin and their corresponding twin. The additive genetics is assumed to be 100% shared between the monozygotic (MZ) or 50% shared between the dizygotic (DZ) twins and is indicated as 1 or 0.5 on the arrow connecting rg and rc. The covariance of age was also included in the model (s). m, male;, f, female.

Figure 2. Statistical parametric map of the average default mode component across all the subjects in resting state. The spatial independent components were decomposed using the GIFT software.

Figure 3. Statistical maps with one sample t-test on the default mode components over subjects (A) and locations of the representative regions for one typical subject (B).

Figure 4. Results of the stochastic DCM. These results are taken from the PCC node. (A, B) show the underlying hidden neuronal and hemodynamic states. The model predictions and prediction error of the BOLD time series are shown in (C).

Figure 5. Results of post hoc model optimization. The model with the highest evidence was the full model (A), which suggested that the full model was the best explanation for our data. (B) shows the conditional parameter estimates over 16 connections. The associated 90% Bayesian confidence intervals are shown as pink bars.

Figure 6. Effective connections of the full model averaged over subjects. The posterior mean values for the coupling parameter is shown along the connections. The headed arrows indicate the direction of the connectivity.

Table 1 The demographic information of the sample and correlation between groups (Mean ± SD).

	mMZ	fMZ	mDZ	fDZ	Total
Sample	13	11	12	10	46
Age	17.45 ± 1.49	17.46 ± 1.18	16.59 ± 1.73	17.01 ± 1.81	17.13 ± 1.58
fMZ	0.033 (0.88)				
mDZ	-0.25 (0.25)	-0.026 (0.91)			
fDZ	-0.026 (0.92)	-0.38 (0.10)	-0.082 (0.73)		

MZ, monozygotic; DZ, dizygotic; m, male; f, female.

Table 2 Additive genetics/common environment/unique environment (A/C/E) model estimates and significant value for the DMN effective connectivity.

r_{MZ}	r_{DZ}	V_A	V_C	V_E	*P* value A/C/E model fit
0.72	0.48	0.54	0.35	0.21	P < 0.0001

V_A, additive genetics variance estimate; V_C, common environment variance estimate;
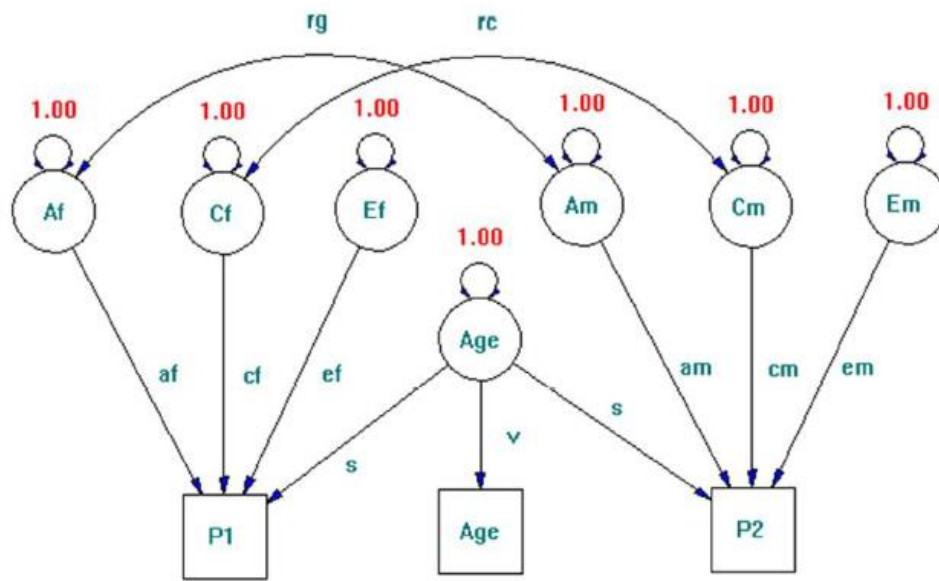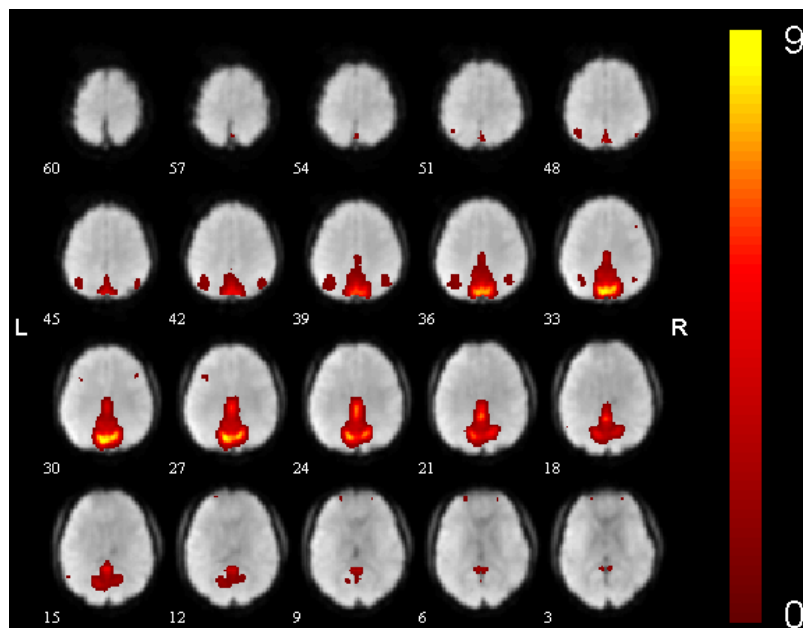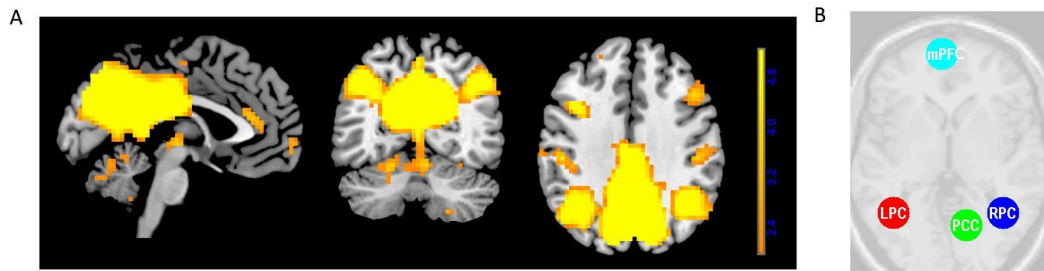
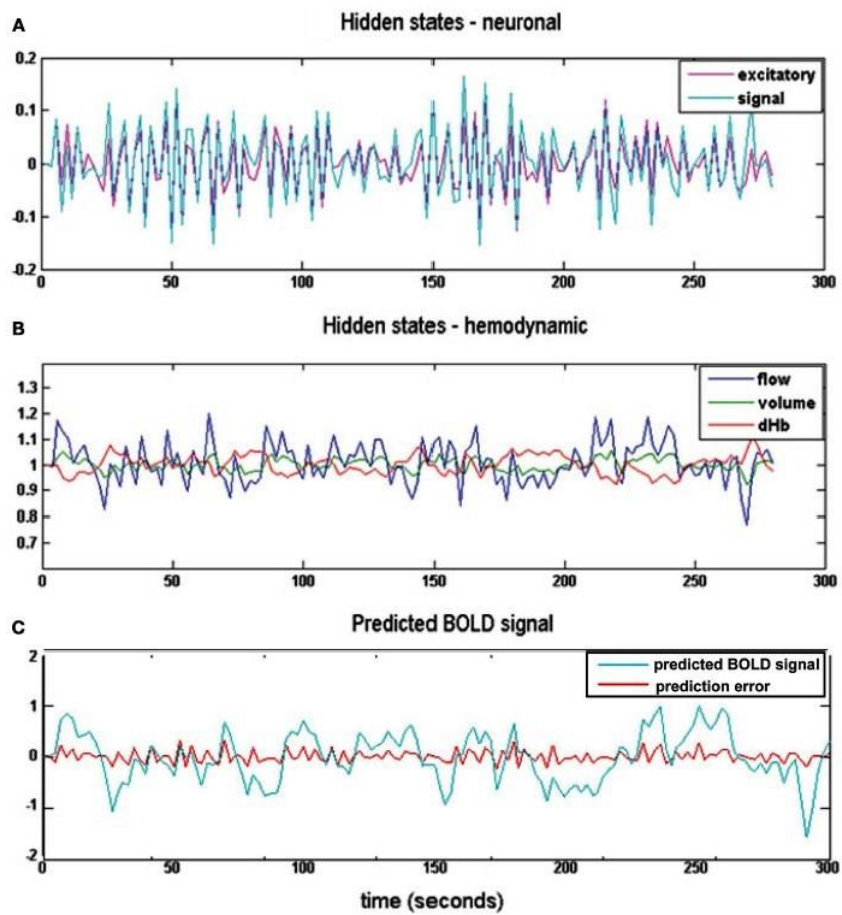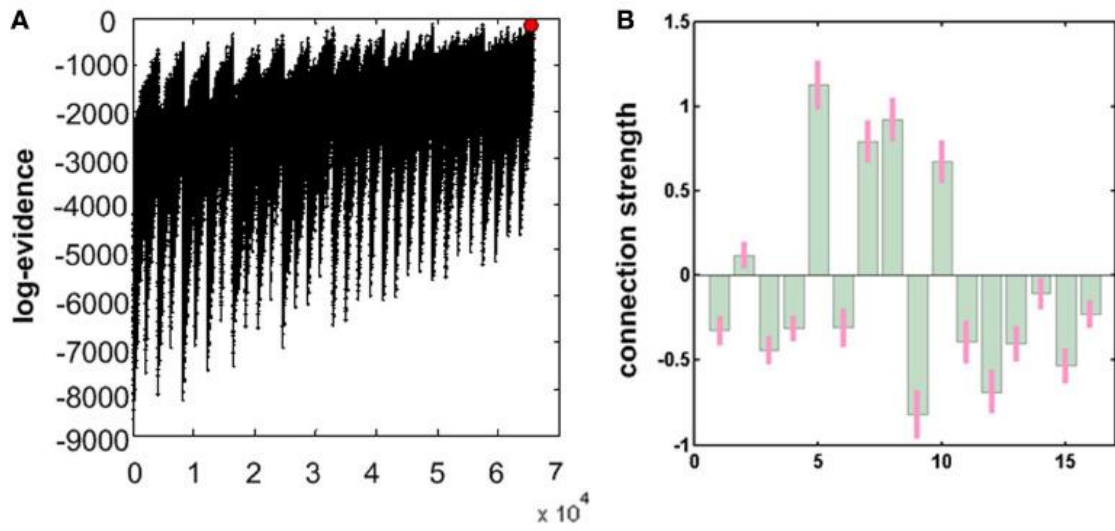V_E, unique environment variance estimate.

Figure 1

Figure 2

Figure 3

Figure 4

Figure 5

Figure 6